Science Progress (2008), 91(4), 377–396 doi: 10.3184/003685008X395517

How to study DNA and proteins by linear dichroism spectroscopy

ALISON RODGER

University of Warwick, Coventry CV4 7AL, UK
E-mail: A.Rodger@warwick.ac.uk

ABSTRACT

The technique of linear dichroism (LD) *is a simple absorbance technique that uses two polarised light beams. Since only oriented molecules show different absorbances for different polarisations,* LD *detects only oriented molecules.*

In aqueous solutions, flow orientation is an attractive orientation methodology as it selects long molecules or molecular assemblies. LD *thus is selective for molecules that are particularly challenging to study by more standard biophysical techniques. In this article, a brief review of the application of* LD *to DNA, DNA–drug systems, DNA–protein enzymatic complexes, fibrous proteins and membrane peptides and proteins is given.*

Keywords: *linear dichroism, DNA, proteins*

Introduction

This article is predicated on the assumption that if we know about the structure of complicated molecules in biological systems then we can begin to work out how they function. With some molecules we can get them to crystallise into regular lattices and determine the structure using X-ray crystallography. However, we are not always sure that the structure the molecule adopts when it is in a regular lattice is the same as when it is in solution interacting with lots of different molecules. In addition, for some classes of molecules crystallography is simply not possible. Such molecules include long DNAs and assemblies of molecules into fibres as well as membrane-bound molecules including membrane proteins. The purpose of this article is to illustrate the advantages and disadvantages of solution-phase flow linear dichroism (*LD*) spectroscopy for structural characterization of solutions of long biomacromolecular molecules. *LD* can also be used for any long not completely flexible

molecules; some carbon nanotube work is reported in references[1,2]. The key to the success of the recent work outlined below was the invention in 2003 of *LD* cells that only required (on a good day) 25 µl of sample[3]; 50 µl makes the experiment easy to do. This was an order of magnitude improvement in sample requirement for *LD* and opened up a wide range of DNA and protein experiments that had been previously impossible. A convenient side-effect of the new cells was that they also reduced artefacts, gave better quality data, and are significantly easier to clean than our previous generations of cells.

Samples for *LD* need to be oriented so the concept of Couette flow is introduced below, followed by a description of linear dichroism and some recent applications, which suggest where the developments will go.

Couette flow

As discussed below *LD* requires the samples to be oriented. If we wish to study molecules in solution, arguably the most relevant state for biological systems, the easiest orientation method is to flow samples. Then as with stirred spaghetti or logs flowing down a stream, molecules with a sufficiently high aspect ratio align in the flow. Flowing a solution through a thin channel is one way to achieve this, however, it is expensive in sample. An alternative is derived from the independent inventions of Maurice Frédéric Alfred Couette and Henry Reginald Arnulph Mallock who in the late 1800s developed a means to measure viscosity based on shearing a liquid between coaxial cylinders[4–7]. Since then there have been many applications of the Couette principle within the engineering and physics communities, the most notable example being Taylor–Couette flow which is a term used to define the flow between rotating cylinders[8–10].

In Couette flow the sample is placed between two cylinders at least one of which rotates. The velocity difference between the two cylinders gives rise to a shear force which orients the samples. Our micro-volume Couette flow cell is illustrated in Figure 1. In this case the outer quartz capillary (whose base is sealed with a plug of Araldite Rapide) rotates and the inner rod, which is suspended vertically from the lid, remains stationary. To avoid artefacts in the *LD* spectra measured (see below) it is essential that the solution remains in the Couette or laminar flow regime. If the cell spins too fast, the flow changes from laminar Couette flow to a series of more complex states, the first of which involves the appearance of Taylor

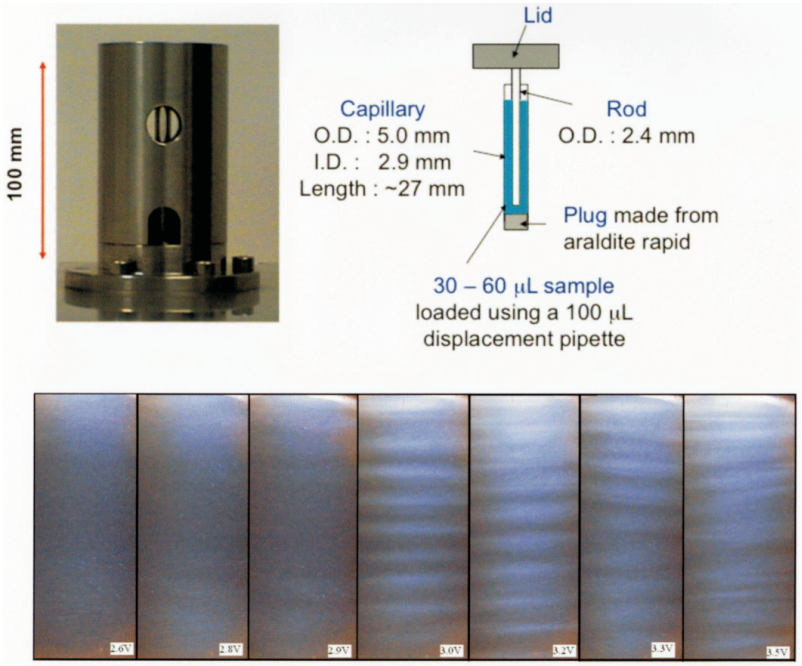

Fig. 1. *Micro-volume Couette flow cell with the states of flow that may be adopted upon increasing rotation speed.*

vortices (vertically stacked toroids of flow around the inner cylinder) and the next involves wavy vortex flow which is exactly what the name says. These can be visualised by introducing a light-reflecting suspended material into an *LD* cell as illustrated in Figure 1 or even more simply by not filling the cell quite enough and pulling air bubbles into the flowing solution. Taylor vortices and wavy vortices are seldom found in our *LD* experiments if the cells are in good condition. The cell used to generate the Figure 1 non-laminar flow is our original *LD* cell whose inner rod is not quite circular in cross-section due to manufacturing difficulties[11].

Linear dichroism spectroscopy

Molecules range in size from about 1 nm to a few hundred nm – all less than the wavelength of visible, near and far ultraviolet (UV) light. Thus we cannot see molecules using light microscopes. An alternative use of light is to shine it on the molecules causing them to absorb photons of the right energy to enable their electrons to

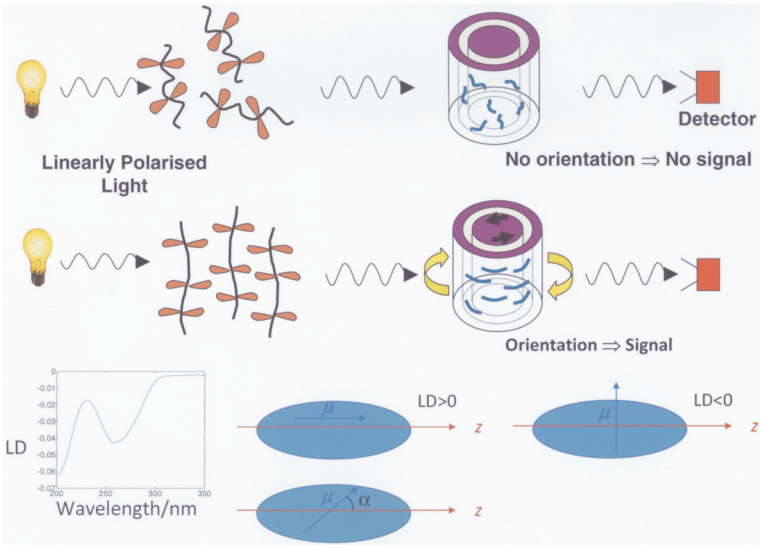

Fig. 2. *Schematic illustration of* LD *spectroscopy.*

jump to a higher energy level. The information about the wavelength of light absorbed and the intensity of the absorption can (often) be interpreted to tell us about the structure of the molecules, since the electrons that 'jump' are the outermost valence electrons which are precisely those that are most involved in forming bonds between atoms to make the molecules in their given structure. The intensity of absorbance of light by a solution of molecules is given by the Beer–Lamber law

$$A = \varepsilon c \ell. \tag{1}$$

where A is absorbance, ε is a wavelength- and molecule-dependent parameter called the extinction coefficient, c is the concentration of the solution and ℓ is the pathlength of the solution through which the light passes.

If we measure the absorbance of light by flow-oriented molecules then we get the same spectrum as for a non-flowing solution unless the light we use is linearly polarised. If we do use linearly polarised light then the electric field of the light only excites electrons that can move parallel to its direction of polarisation as illustrated in Figure 3. By using two linearly polarised light beams and taking the difference in their absorbance signals, we completely remove the contributions from the unoriented molecules and just collect the linear dichroism signal as illustrated in Figure 3.

$$LD = A_{//} - A_{\perp}. \tag{2}$$

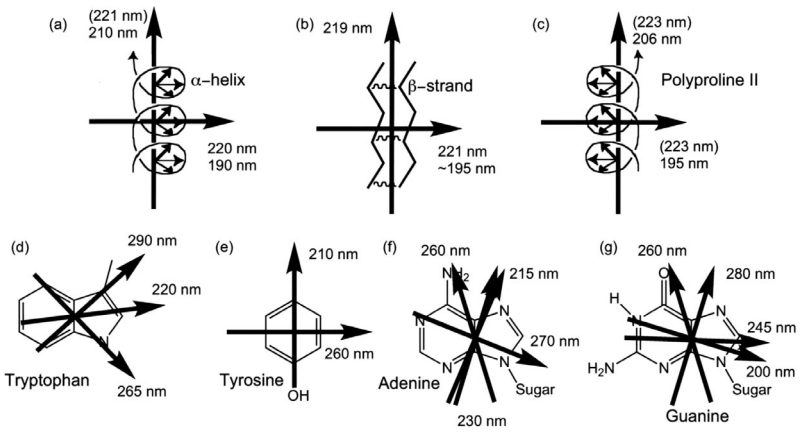

Fig. 3. *Transition polarisations (indicated by arrows) of relevance for biomacromolecules (see ref. 29).*

The invisible unoriented molecules are typically small molecules that are in the solution either as by-products from making a long flow orientable molecule or else as additions to keep it stable at a given pH *etc*.

By convention the parallel direction (//) in equation (2) is taken to be along the flow direction, the perpendicular direction ($\perp$) orthogonal to the flow direction and the light propagates perpendicular to both // and $\perp$.

Different transitions of the electron density in a molecule have different polarisations (their direction of net motion), so some transitions end up with a positive *LD* and some with a negative *LD*. When we plot *LD* as a function of wavelength, a spectrum such as that illustrated in Figure 2 results. Some transition polarisations of relevance for biomacromolecules are shown in Figure 3^{2-15}. The reduced linear dichroism LD^r is a convenient pathlength- and concentration-independent summary of *LD* data for quantitative analysis:

$$LD^r = \frac{LD}{A} = \frac{A_{//} - A_{\perp}}{A} = \frac{3}{2} S(3\cos^2\alpha - 1) \qquad (3)$$

where α is the angle between the transition's polarisation and the direction of flow (Figure 3) and S is the extent of orientation of the sample. $S = 0$ for unoriented samples and 1 for perfectly oriented ones. So $LD = 0$ if a transition is oriented at 54.7° to the direction of flow, positive if it is more parallel to the flow than this and negative if it is less parallel.

How linear dichroism can be used to understand what molecules are doing

Much of the flow linear dichroism literature relates to nucleic acids. The DNA work published before the early 1990's has been superbly reviewed by Nordén, Kubista and Kuruscev in[16]. An earlier linear dichroism review by Nordén is more general in subject matter[17]. Here we shall use some examples of DNA and DNA–drug systems to show how to use *LD* to help work out what molecules are doing and then give some other examples of how linear dichroism can be used to study fibrous and membrane proteins. The intent here is to be illustrative rather than comprehensive, though the references cited open up a literature trail that should lead to most available literature.

DNA and DNA-small molecule complexes

From a spectroscopic point of view DNA is a spiral staircase of aromatic molecules, the nucleotide bases. In the most common form of DNA, B-DNA, the staircase is right handed and the steps are perpendicular to the helix axis, which is also the orientation axis. As the $\pi-\pi$ transitions of the aromatic bases are all polarised within the plane of the steps of the staircase as illustrated in Figure 4, the absorbance is perpendicular to the orientation axis, so we expect the *LD* spectrum to be very similar to an upside-down DNA absorbance spectrum as shown in Figure 4. The magnitude of the *LD* depends on the concentration of the sample and how fast the solution is flowing or equivalently how fast the Couette cell is spinning. As long as the flow remains laminar, faster is usually better (Figure 4).

When we add small molecule ligands to the DNA solution we expect to see them in the *LD* spectrum if and only if they are bound to the DNA. Ethidium bromide (Figure 5a) is often used as a DNA stain; it is a planar aromatic molecule that intercalates (sandwiches) between the DNA base pairs. Its transitions are therefore also perpendicular to the helix axis and its *LD* signals are the same sign as that of the DNA bases. Hoechst, another DNA stain, is, by way of contrast, a minor groove binder and so its long axis polarised transitions are expected to lie at $\sim 45^\circ$ to the helix axis (Figure 5b). Referring back to Equation (3) and using the data in Figure 5b, assuming the DNA bases lie at an angle of 86°, it follows that $S = 0.030$, and the long axis of Hoechst actually makes an angle of 47° with the DNA helix axis. Thus, for new ligands their orientation on DNA can be determined as long as the

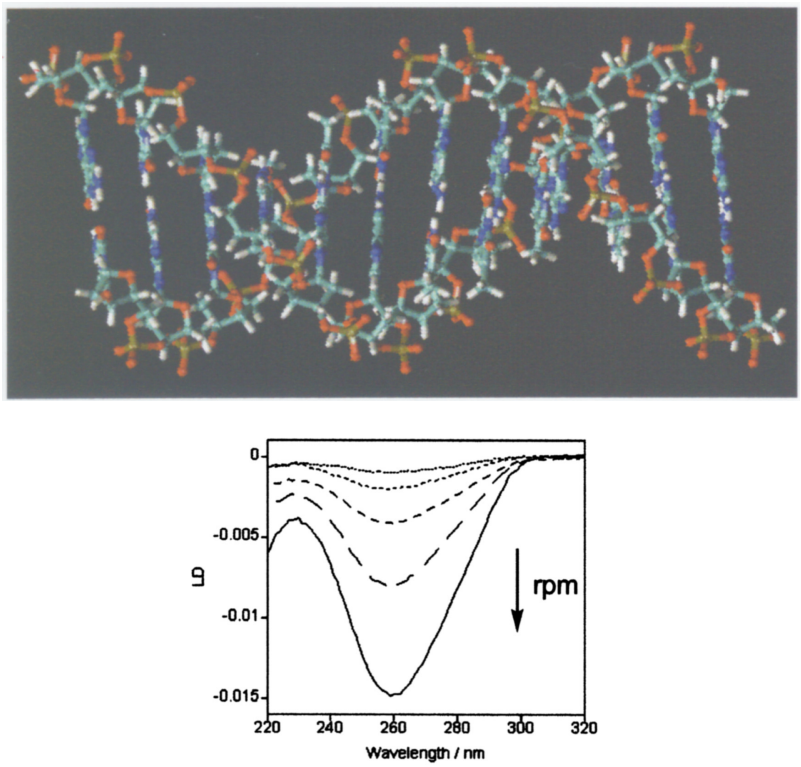

Fig. 4. *Schematic of DNA illustrating that the bases are perpendicular to the DNA helix axis. DNA* LD *spectrum as a function of increasing rotation speed (560 rpm to 4800 rpm).*

polarisations of the transitions within the ligand are known and the orientation parameter, *S*, of the DNA is known.

Many DNA-binding ligands have absorbance signals at 260 nm so their own *LD* signals overlay that of the DNA; thus we cannot simply use the 260 nm *LD* to determine *S*. Hoping *S* is the same for DNA with and without a ligand can be dangerous as Figure 6 shows. In this case the bimetallo iron helicate (illustrated in Figure 6 binds to the DNA and also intramolecularly coils it up[18]. We have recently used *LD* to probe the orientation of a new ruthenium metal complex on DNA and to see whether it coils DNA. The data for $\Delta,\Delta-[Ru_2(bpy)_4L^1]^{4+}$ (Figure 6) are consistent with it binding to DNA outside the grooves and wrapping the DNA about it[19]. This compound showed little biological activity in cell tests, so either the DNA can cope with this level of structure perturbation by a ligand or the molecule never gets as far as the DNA in the cell.

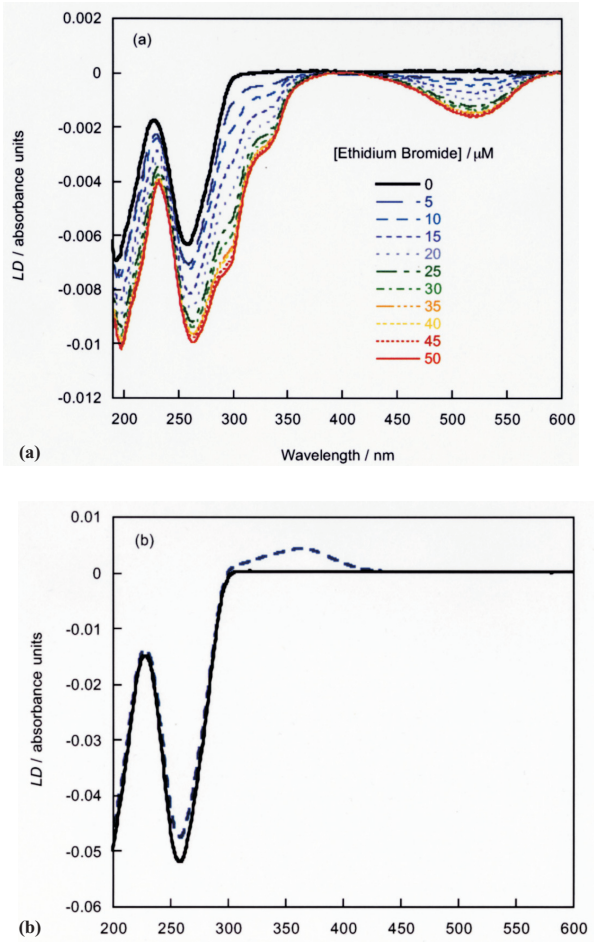

Fig. 5. **(a)** LD *of calf thymus DNA (200* μ*M in base) with increasing amounts of the intercalator ethidium bromide.* **(b)** LD *of calf thymus DNA (1000* μ*M in base) with the grove binder Hoechst 33258 (50* μ*M).*

Restriction enzyme action on DNA

Type II restriction endonucleases are enzymes that recognize and cleave specific DNA sequences. They have evolved to protect prokaryotic organisms from invasion by foreign DNA: their own DNA is protected by a specific DNA methylation patterns (N4 or C5 methylation of cytosine or N6 methylation of adenine) whereas the foreign DNA is not so protected and is therefore susceptible to cleavage (restriction) by the host enzyme[20]. There are thousands of restriction enzymes that have been identified to date. They are also

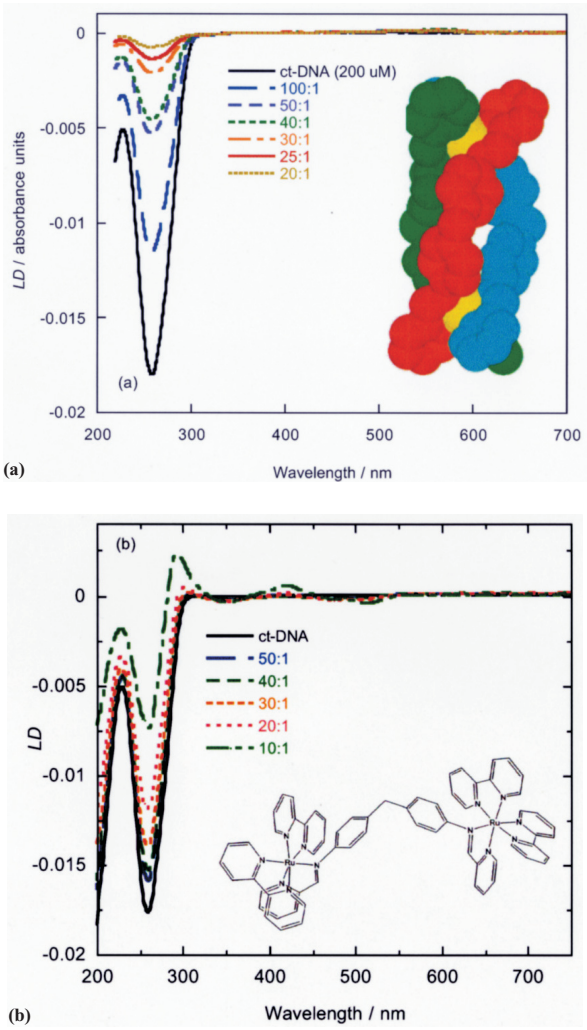

Fig. 6. **(a)** LD *spectra of calf thymus DNA (200 μM) with and (−)-*$[Fe_2L_3]^{4+}$ *(illustrated) bound to it.* $[Fe_2L_3]^{4+}$ *is illustrated in the inset.* **(b)** LD *spectra of calf thymus DNA (200 μM) with* Δ, Δ-$[Ru_2(bpy)_4L^1]^{4+}$ *(illustrated).*

extremely important tools for the molecular biologist as they are used in many techniques that require DNA manipulation and have applications in, for example, diagnostics and recombinant protein production[21]. The normal methodology is to leave the DNA and the restriction enzyme incubating at a chosen temperature for long enough to hope it has all reacted. This is sometimes checked by gel electrophoresis and sometimes not. There are other methods of

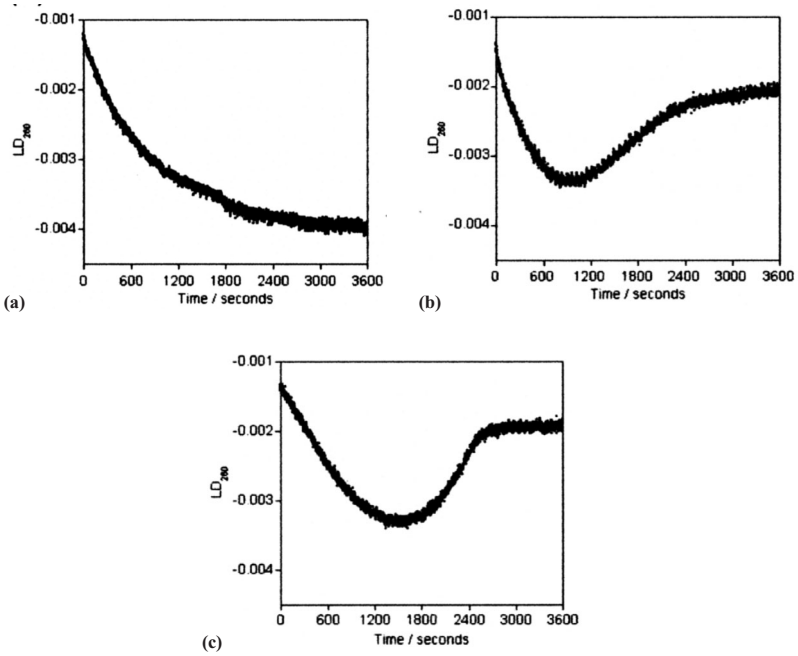

Fig. 7. LD *of restriction digests of a circular, super-coiled plasmid, showing changes in DNA length* (LD *magnitude*) *as a function of time.* **(a)** *Plasmid was digested with* Eco*RI, which has a single cut site in the DNA sequence.* **(b)** *Plasmid digestion with* Eag*I, which has two cut sites in the DNA sequence.* **(c)** *Plasmid digestion with* Bst*Z17I, which also has two cut sites in the DNA sequence.*

monitoring the reaction but they involve either extra chemical labelling of the DNA with a fluorophore[22] or require the DNA to become single stranded after cleavage[23]. *LD* is the ideal technique to probe the activity of a restriction enzyme since if a plasmid (circular supercoiled piece of DNA) is cleaved, it unravels, gets longer and orients better in flow. If a linear piece of DNA is cut, then it will get shorter and the *LD* signal is expected to be reduced in magnitude.

Three examples of the effect of a restriction enzyme on DNA are shown in Figure 7. The enzyme EcoRI has a single recognition site in the plasmid and as such is expected produce a linear DNA molecule. Figure 7 shows an increase in the magnitude of the negative LD_{260} which is consistent with an increase in orientation after linearization of the plasmid, as predicted. The effect of an enzymes with two cleavage sites in the plasmid DNA is shown in the *LD* traces of Figures 7b and 7c where the enzymes *Eag*I and *BstZ*17I were used, respectively. In both cases there is an initial

increase in the magnitude of the negative *LD* signal at earlier time showing the linearization of the plasmid followed by a decrease when the second cut takes place.

Cytoskeletal proteins

The cytoskeleton is a dynamic scaffold or skeleton that is present in the cytoplasm of all cells. It maintains cell shape, often protects the cell, enables cellular motion, and plays important roles in both intracellular transport of *e.g.* vesicles and organelles and in cell division. The cytoskeleton in both prokaryotic and eukaryotic cells is dependent on the rapid assembly and disassembly of polymers whose monomeric units are themselves folded proteins. The structures of the monomers change little if at all when they form a fibre. Although we know a lot about the cytoskeleton there is also a lot that we do not know. It is a challenge to study as it is dynamic and large. We have recently found that *LD* can be used to 'see' properties of cytoskeletal fibres that other techniques miss. The possibilities of *LD* spectroscopy can be illustrated by looking at the bacterial homologue of tubulin, FtsZ and tubulin itself.

The tilting of guanine in FtsZ fibres

FtsZ is a soluble globular protein that, prior to cell division, polymerises to form the so-called Z-ring which grabs the cell membrane (via other proteins). The Z-ring then contracts and pulls in the cell membrane ultimately enabling one cell to divide into two daughter cells (Figure 8). FtsZ polymerisation to form protofilaments (a stack of monomer units) requires the nucleic acid GTP (guanine triphosphate) and Mg^{2+} to be present. One GTP ends up being sandwiched between each successive pair of FtsZ monomers. The protofilament *LD* spectrum is given in the 0 mM Ca^{2+} spectrum of Figure 8. In an *LD* cell we can mimic the Z-ring formation by making FtsZ protofilaments bundle together using dications such as Ca^{2+}.[24] When this happens, the 244–266 nm region of the spectrum changes from negative to positive. By studying the *LD* signal of the guanine, one can see that the bundling process results in the guanine chromophores of the GTPs (which are between each pair of monomer units) tilting as shown by the positive peak that appears at 250 nm. By considering the polarisations of the guanine transitions (Figure 3), one can deduce that the G in the protofilaments is more or less perpendicular to the fibre axis, whereas in the bundles the G's have been tilted as suggested in

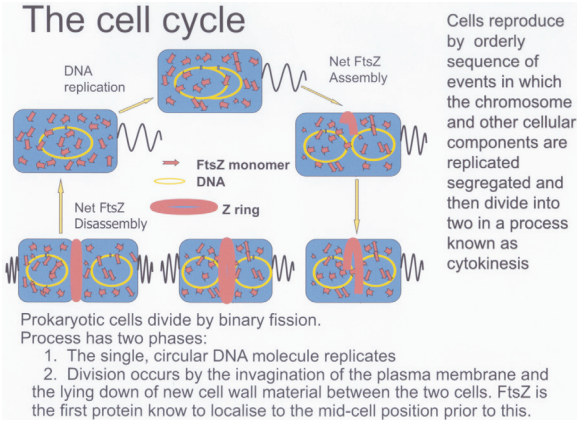

(a)

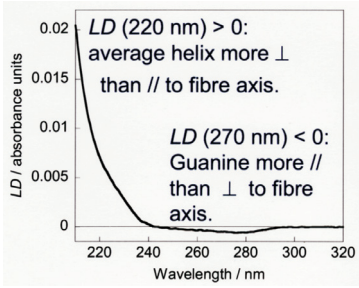

(b)

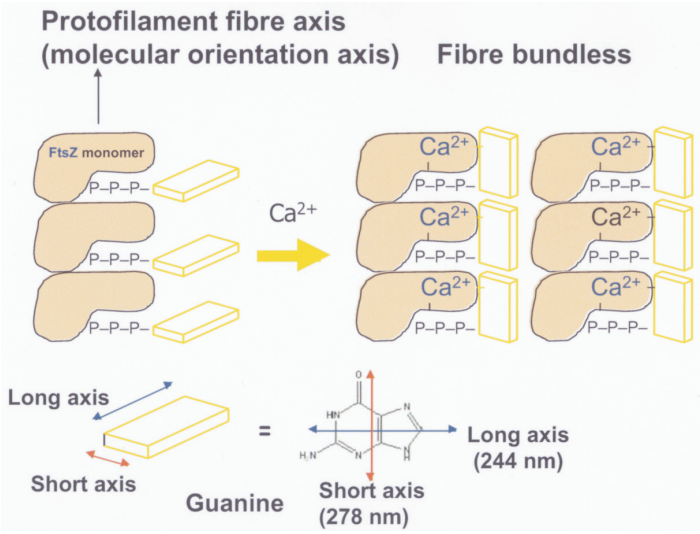

(c)

Fig. 8. **(a)** *Schematic of the prokaryotic cell cycle.* **(b)** *The FtsZ (11 μM, one minute after adding GTP (0.2 mM) in 50 mM MES buffer pH 6.5, 10 mM $MgCl_2$ and 50 mM KCl) protofilament* LD *spectrum.* **(c)** *Schematic of protofilaments and bundles showing G reorientation.*

the schematic of Figure 8. This is a fascinating insight since the main mechanism of control of the FtsZ fibres and the Z-ring appears to be GTP hydrolysis to GDP (guanine diphosphate), whereupon the fibres bend (Figure 8). When the protofilaments bundle then the hydrolysis slows down or even stops, suggesting the FtsZ cannot catalyse the reaction when the Gs have been tilted. The protein YgfE performs the same role as the calcium ions but at more biologically realistic concentrations[25].

Microtubule assembly and disassembly

Because monomeric FtsZ and tubulin have no flow *LD* signal, *LD* is the ideal technique to follow the kinetics of their fibre assembly and disassembly. Tubulin assembles into the so-called microtubules that play a role in moving molecules and organelles about and most importantly help control the processes that ensures two daughter cells each get one complete set of chromosomes. Microtubules grow during mitosis and attach to newly replicated chromosomes forming the mitotic spindle. Depolymerisation then occurs and sister chromatids move to opposite poles of the cell. As with FtsZ, a GTP molecule (Figure 3) is sandwiched between each monomer when they assemble into the microtubule. Because of their significance to the health of the cell, microtubules are very attractive drug targets. However, as with FtsZ, traditional structural techniques struggle to probe how potential drugs affect the microtubule structure. *LD* is particularly attractive in this instance as it is sensitive only to the assembled microtubules. Figure 9a shows the kinetics of polymerisation and depolymerisation of tubulin[26]. What is not apparent from the *LD* data is that the microtubules are constantly polymerising at one end and depolymerising at the other as long as a supply of GTP is present. So we are seeing first net polymerisation when GTP is present and then a net depolymerisation after the GTP is exhausted. The polymerisation in the absence and presence of paclitaxel (more commonly known as the anticancer drug taxol) illustrates (Figure 9b) the stabilisation effect of taxol on the microtubules – which inhibits cell division. Colchicine (which is used in the treatment of gout), by way of contrast, results in net tubulin depolymerisation by preventing the polymerisation reaction at one end of the polymer but allowing the depolymerisation one at the other end.

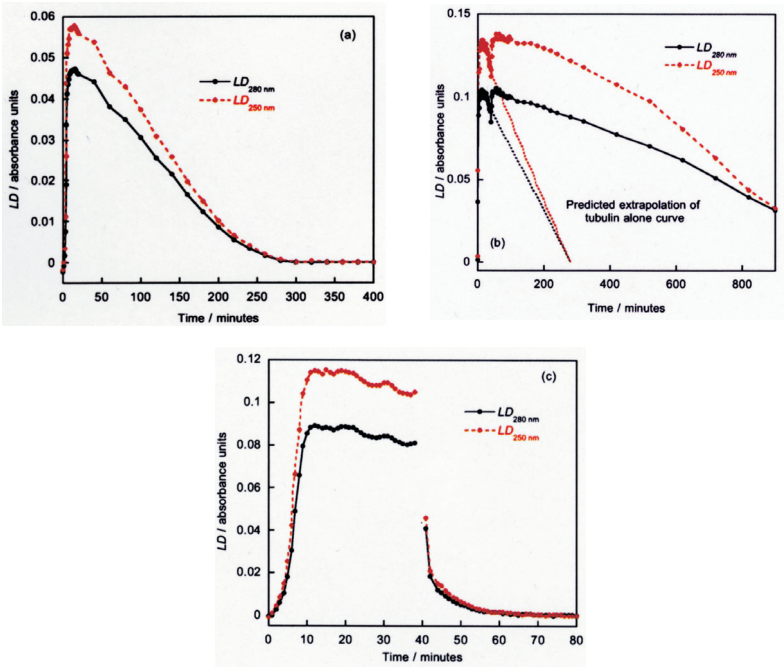

Fig. 9. *The kinetics of polymerisation and depolymerisation at 37°C of* **(a)** *tubulin (28 μM),* **(b)** *tubulin in the presence of paclitaxel, and* **(c)** *tubulin in the presence of colchicine.*

Membrane proteins and peptides

Membrane proteins and peptides are peripherally associated with or embedded within a cell's membranes. They play key roles in cells and are directly linked, among other things, to viral infection, cancer, diabetes, and heart disease. Some membrane proteins act as channels to transport species into and out of cells or organelles, others may disrupt the membrane to which they bind, yet others transmit signals by changing their structure upon ligand binding. Membrane proteins are therefore important drug targets and also drug candidates but we have only a very limited understanding of their structure, function, and intermolecular interactions. Membrane peptides and proteins are so challenging to study because the normal environment of a membrane protein includes a lipid bilayer and its associated surface and integral small molecules and proteins, all solvated by an aqueous solution also containing a wide range of molecules. The lipids of the bilayer also vary significantly in structure depending on what cell or organelle one is considering.

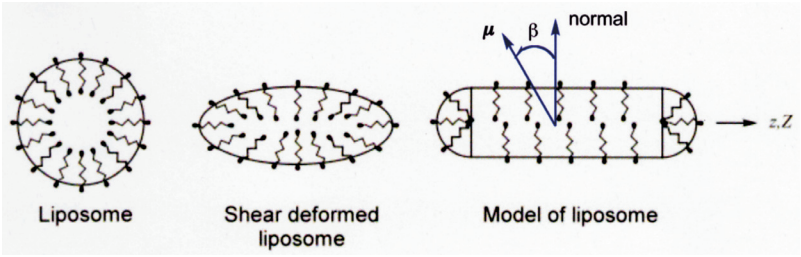

Fig. 10. *Schematic illustration of the effect of flow on a unilammellar liposome illustrating the geometry used to analyse data.*

Membrane proteins have been studied by *LD* for a long time using more-or-less dried films and squeezed gel methodologies[27]. Nordén *et al*.[28] opened up the possibilities for solution phase lipid membrane *LD* by showing that small molecules such as pyrene could be flow oriented in unilamellar liposomes – model membrane systems with a single bilayer of lipid enclosing a central space. We[29] showed this could be extended to proteins and peptides and since then have been developing the use of *LD* to study peptides and proteins inserted in liposomes as a method for probing their structure and kinetics of insertion. The possibilities are illustrated below with reference to bateriorhodopsin, probably the most-studied membrane protein, and gramicidin, a similarly popular membrane-inserting peptide. In interpreting membrane *LD* data one must note that the geometry of the liposome experiment is different from that of long polymers since the flow direction creates the long axis of the liposome (Figure 10) but the membrane normal (which is perpendicular to the long axis of the liposome) is the molecular orientation direction. The equation analogous to equation (3) for liposome systems is therefore:[28,29]

$$LD^r = \frac{LD}{A_{iso}} = \frac{3S}{4}\left(1 - 3\cos^2\beta\right) \tag{4}$$

where β is the angle between the lipid normal and the long axis of the molecule as illustrated in Figure 10.

Bacteriorhodopsin

Bacteriorhodopsin (BR) is a membrane protein found in the purple membrane of Halobacteria[30]; it is a 248 residue protein and includes a covalently bound retinal (a vitamin A derivative) chromophore (Figure 11). BR captures light energy (using the

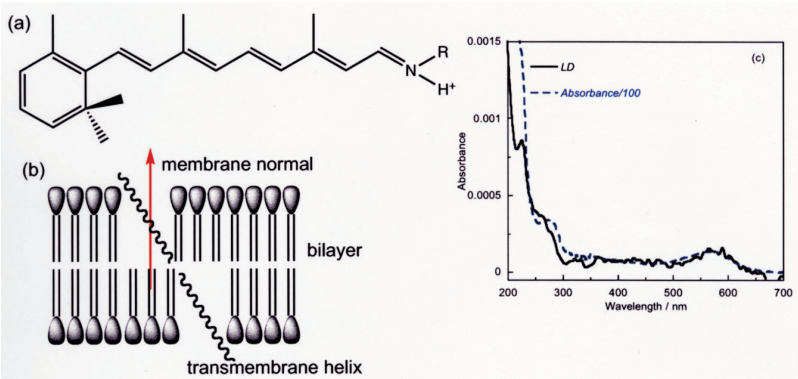

Fig. 11. **(a)** *All-trans retinal converted to the Shiff base.* **(b)** *Schematic illustration of the average orientation of the transmembrane helices of BR in the liposome bilayer deduced from the* LD. **(c)** *A flow* LD *spectrum of BR (0.2 mg ml*$^{-1}$*) inserted into syabean lipid liposomes (0.5 mg ml*$^{-1}$*).*

retinal chromophore) and uses it to move protons across the membrane out of the cell. The resulting proton gradient is subsequently converted to chemical energy by the cell. Each BR has seven *trans* membrane helices, three of which in the crystal have their axis at $\sim 70^\circ$ to the lipids and the remaining 4 are parallel to the lipids[31]. The long axis of the retinal lies at $\sim 69^\circ$ to the lipids in the crystal. A flow *LD* spectrum of BR inserted into liposomes is shown in Figure 11. The 570 nm peak is due to a long axis polarised transition of the retinal chromophore; the broad peak in the near UV region (260–290 nm) is due to the transitions of the protein aromatic side chains (dominated by the indole chromophore of the tryptophan residues); the peak observed in the far UV region (220– $\sim$230 nm) is due to the peptide $n \rightarrow \pi^*$ transition of the amide groups; and the lowest wavelength bands shown are $\pi \rightarrow \pi^*$ transitions. If we assume the retinal is at 69° to the lipids as in the crystal, equation (4) gives $S \sim 0.05$. It then follows that the tryptophan transitions are oriented at: $\beta(L_a, 270\,\text{nm}) \sim 60^\circ$ and $\beta(Lb, 287\,\text{nm}) \sim 65^\circ$. This is consistent with the X-ray structure which show that the retinal is sandwiched by tryptophan residues[30]. The protein backbone *LD* spectrum, however, shows a positive maximum at 220 nm ($n \rightarrow \pi^*$) and a negative maximum at $\sim$213 nm ($\pi \rightarrow \pi^*$) from which it follows that the $n \rightarrow \pi^*$ transition (which is polarised perpendicular to the α–helix long axis, Figure 3) is $\sim 58^\circ$ from the average lipid direction. Thus the average orientation of the transmembrane helices is $\sim 30^\circ$ from the membrane normal. This value suggests

that the protein is less rigidly held in a liposome than when dried or crystallised – which is not entirely surprising.

Gramicidin insertion

Many naturally occurring peptides show antibiotic properties. Some of them act by inserting into the bacterial cell membrane and disrupting its function in some way, the most dramatic being by causing the cell membrane to lose its structural integrity so it no longer encapsulates the cell. The kinetics of such processes can be studied using techniques such as fluorescence and circular dichroism. Fluorescence given an indication of the hydrophobicity of the environment of any tryptophans in the peptide and may also give an indication of any size changes (since scattered photons register as an unstructured fluorescence spectrum). Circular dichroism gives a direct read-out of any changes in secondary structure of the peptide such as its folding into an α-helix. However, neither technique indicates whether the peptide has actually inserted into the membrane. We have been developing UV *LD* to study peptides and proteins inserted in liposomes as a method for probing their structure and kinetics of insertion[29,32,33]. For example if a peptide folds into an α-helix on the surface of the membrane, its 222 nm $n-\pi^*$ transition will be oriented preferentially pointing down into the membrane, thus giving rise to a negative *LD*. If the helix then inserts, the *LD* at 222 nm will change to positive as the transition will be preferentially oriented parallel to the liposome long axis as illustrated in Figure 12. Alternatively, if the peptide folds and inserts in one simultaneous step, one would see a random coil circular dichroism spectrum converting to a helical one on exactly the same time scale as the appearance of the positive *LD*. This is in fact precisely what we found for Gramicidin dissolved in TFE when it was added to small unilamellar phosphatidylcholine vesicles in water[32]. First the tryptophans bury themselves in the hydrophobic membrane environment (the fluorescence shifts to shorter wavelength), then the gramicidin forms itself into the double helical pore form (as shown by the shape of the *CD* spectrum). *LD* kinetics shows (Figure 12) that the peptide inserts simultaneously with the formation of the helix rather than the previously assumed mechanism whereby it folded then inserted. At higher gramicidin concentrations and longer times the data show an increasing in light scattering and loss of *LD* signal as the liposomes burst apart.

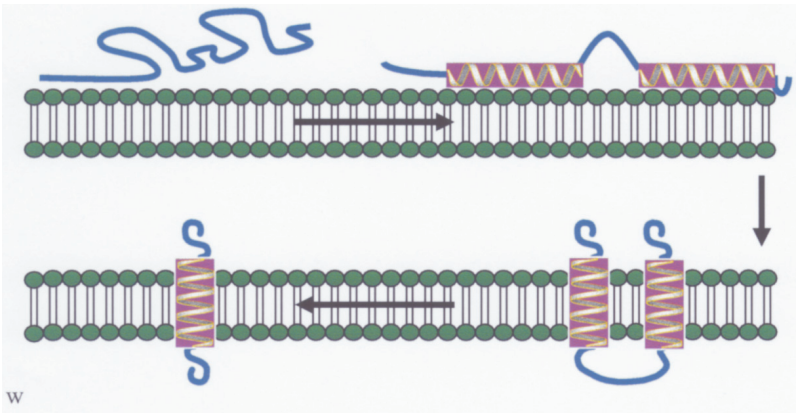

Fig. 12. **(a)** *Schematic illustration of two helices folding on the surface of a lipid bilayer and then inserting. Cleavage to a single helix is also illustrated.* **(b)** *Rate of folding and insertion of gramicidin (50* μg *ml*$^{-1}$ *in 10% TFE v/v) into liposomes (1800* μg *ml*$^{-1}$ *phosphatidyl choline).*

LD to screen antibiotic peptides

Having developed the methodology for probing the insertion of peptides into membranes the next phase of this programme is to use it to screen peptides for antibacterial (or antifungal) activity and selectivity in that action. By creating model membrane systems that mimic the membranes of bacteria and their hosts we can determine whether a given peptide binds or not, whether it inserts or not and what its effect on the membrane is. By comparing the effect on host and bacterial membrane we can ascertain whether any level of selectivity is to be expected since any membrane disrupting antibiotic needs to only disrupt the target membrane rather than that of the host, which needs to remain alive and healthy or else the role of the antibacterial agent is null and void.

Conclusion

The technique of linear dichroism is a simple absorbance technique using two polarised light beams. Since only oriented molecules show different absorbances for different polarisations, *LD* detects only oriented molecules. This means that we can study one molecule against a background of many absorbing species – as long as the molecule we are interested in can be oriented. In aqueous solutions, flow orientation is an attractive orientation methodology as it selects longs molecules or molecular assemblies (or ones that can be induced to adopt a high aspect ratios by the

flow, such as liposomes). *LD* thus is selective for molecules that are particularly challenging to study by more standard biophysical techniques. In this article, a brief review of the application of *LD* to DNA, DNA–drug systems, DNA–protein enzymatic complexes, fibrous proteins and membrane peptides and proteins has been given.

References

1. Rajendra, J., Baxendale, M., Dit Rap, L.G. and Rodger, A. (2004) Flow linear dichroism to probe binding of aromatic molecules and DNA to single walled carbon nanotubes. *J. Am. Chem. Soc*., **126**, 11182–11188.
2. Rajendra, J. and Rodger, A. (2005) The binding of single stranded DNA and PNA to single walled carbon nanotubes probed by flow linear dichroism. *Chem. Eur. J*., **11**, 4841–4848.
3. Marrington, R., Dafforn, T.R., Halsall, D.J. and Rodger, A. (2004) Micro volume Couette flow sample orientation for absorbance and fluorescence linear dichroism. *Biophys. J*., **87**, 2002–2012.
4. Couette, M. (1890) *Ann. Chim. Phys*., **6**, 433–510.
5. Mallock, A. (1988) *Proc. R. Soc. Lond*., 1888, **45**, 126.
6. Mallock, A. (1896) *Phil. Trans. R. Soc. Lond., Ser., A*, 1896, **187**, 41.
7. Donnelly, R.J. *Phys. Today*, 1991, November, 32–39.
8. Taylor, G.I. (1923) *Proc. R. Soc. Lond. Ser. A*, **223**, 289–343.
9. Taylor, G.I. (1936) *Proc. R. Soc. Lond. Ser. A*, **157**, 546–564.
10. Taylor, G.I. (1936) *Proc. R. Soc. Lond. Ser. A*, **157**, 565–578.
11. Rodger, A. (1993) *Meth. Enzymol*., **226**, 232–258.
12. Rodger, A., Rajendra, J., Marrington, R., Ardhammar, M., Nordén, B., Hirst, J.D., Gilbert, A.T.B., Dafforn, T.R., Halsall, D.J., Woolhead, C.A., Robinson, C., Pinheiro, T.J., Kazlauskaite, J., Seymour, M., Perez, N. and Hannon, M.J. (2002) *Phys. Chem. Chem. Phys*., **4**, 4051–4057.
13. Albinsson, B. and Nordén, B. (1992) *J. Phys. Chem*., **96**, 6204–6212.
14. Holmen, A., Broo, A., Albinsson, B. and Nordén, B. (1997) *J. Am. Chem. Soc*., **119**, 12240–12250.
15. Dafforn, T.R., Rajendra, J., Halsall, D.J., Serpell, L.C. and Rodger, A. (2004) *Biophys. J*., **86**, 404–410.
16. Nordén, B., Kubista, M. and Kuruscev, T. (1992) *Q. Rev. Biophys*., **25**, 51–170.
17. Nordén, B. (1978) *Appl. Spectrosc. Rev*., **14**, 157–248.
18. Meistermann, I., Moreno, V., Prieto, M.J., Molderheim, E., Sletten, E., Khalid, S., Rodger, P.M., Peberdy, J., Isaac, C.J., Rodger, A. and Hannon, M.J. (2002) Intramolecular DNA coiling mediated by metallo-supramolecular cylinders: differential binding of P and M helical enantiomers. *Proc. Natl Acad. Sci. USA*, **99**, 5069–5074.
19. McDonnell, U., Hicks, M.R., Hannon, M.J. and Rodger, A. (2008) DNA binding and bending by dinuclear complexes comprising ruthenium polypyridyl centres linked by a bis(pyridylimine) ligand. *J. Inorg. Biochem*., **102**, 2052–2059.

20. Pingoud, A., Fuxreiter, M., Pingoud, V. and Wende, W. (2005) Type II restriction endonucleases: structure and mechanism. *Cell. Mol. Life Sci*., **62**, 685–707.
21. Sambrook, J., Fritsch, E.F. and Maniatis, T. (1989) *Molecular Cloning: A Laboratory Manual*. Cold Spring Harbor Laboratory Press, New York.
22. Kettling, U., Koltermann, A., Schwille, P. and Eigen, M. (1998) Real-time enzyme kinetics monitored by dual-color fluorescence cross-correlation spectroscopy. *Proc. Natl. Acad. Sci. USA*, **95**, 1416–20.
23. Waters, T.R. and Connolly, B.A. (1992) Continuous spectrophotometric assay for restriction endonucleases using synthetic oligodeoxynucleotides and based on the hyperchromic effect. *Analyt. Biochem*., **204**, 204–209.
24. Marrington, R., Small, E., Rodger, A., Dafforn, T.R. and Addinall, S.G. (2004) FtsZ fibre bundling is triggered by a calcium-induced conformational change in bound GTP. *J. Biol. Chem*., **47**, 48821–48829.
25. Small, E., Marrington, R., Rodger, A., Scott, D.J., Sloan. K., Roper, D., Dafforn, T.R. and Addinall, S.G. (2007) FtsZ polymer-bundling by the *Escherichia coli* ZapA orthologue, YgfE involves a conformational change in bound GTP. *J. Mol. Biol*., **369**, 211–221.
26. Marrington, R., Seymour, M. and Rodger, A. (2006) A new method for fibrous protein analysis illustrated by application to tubulin microtubule polymerisation and depolymerisation. *Chirality*, **18**, 680–690.
27. van Amerongen, H. and van Grondelle, R. (1989) Orientation of the bases of single-stranded DNA and polynucleotides in complexes formed with the gene 32 protein of bacteriophage T4. A linear dichroism study. *J. Mol. Biol*., **209**, 433–445..
28. Ardhammar, M., Mikati, N. and Nordén, B. (1998) Chromophore Orientation in Liposome Membranes Probed with Flow Linear Dichroism. *J. Am. Chem. Soc*., **120**, 9957–9958.
29. Rodger, A., Rajendra, J., Marrington, R., Ardhammar, M., Nordén, B., Hirst, J.D., Gilbert, A.T.B., Dafforn, T.R., Halsall, D.J., Woolhead, C.A., Robinson, C., Pinheiro, T.J., Kazlauskaite, J., Seymour, M., Perez, N. and Hannon, M.J. (2002) Flow oriented linear dichroism to probe protein orientation in membrane environments. *Phys. Chem. Chem. Phys*., **4**, 4051–4057.
30. Oesterhelt, D. and Stoeckenius, W. (1971) Rhodospin-like protein from the purple membrane of *Halobacterium halobium*. *Nature New Biol*., **233**, 149–152.
31. Henderson, R., Baldwin, J.M., Ceska, T.A., Zemlin, F., Beckmann, E. and Downing, K.H. (1990) Model for the structure of bacteriorhodopsin based on high-resolution electron cryo-microscopy. *J. Mol. Biol*., **213**, 899–929.